Journal of Orthopaedic Translation 28 (2021) 148–158

Contents lists available at ScienceDirect

Journal of Orthopaedic Translation

journal homepage: www.journals.elsevier.com/journal-of-orthopaedic-translation

Tyloxapol inhibits RANKL-stimulated osteoclastogenesis and ovariectomized-induced bone loss by restraining NF-κB and MAPK activation

Wen Guo [a,b,1], Haijun Li [b,1], Yan Lou [c,1], Yue Zhang [c,1], Jia Wang [d], Ming Qian [c,****], Haifeng Wei [c,***], Jianru Xiao [c,**], Youjia Xu [a,e,*]

[a] Department of Orthopedics, The Second Affiliated Hospital of Soochow University, Suzhou, 215004, China
[b] Department of Orthopedics, Taizhou People's Hospital, Taizhou, 225300, Jiangsu, China
[c] Orthopaedic Oncology Center, Department of Orthopaedics, Changzheng Hospital, Second Military Medical University, Shanghai, 200000, China
[d] School of Public Health, Shandong First Medical University & Shandong Academy of Medical Sciences, Taian, 271016, Shandong, China
[e] Osteoporosis Institute, Soochow University, Suzhou, 215004, China

ARTICLE INFO

Keywords:
Tyloxapol
Osteoporosis
Osteoclast
Osteoblast
Nuclear factor kappa-B (NF-κB)
Mitogen-activated protein kinase (MAPK)

ABSTRACT

Objective: Tyloxapol is a non-ionic surfactant with diverse pharmacological effects including anti-inflammatory, anti-malignant tumor and antioxidant activities. However, the effect of tyloxapol on osteoclastogenesis has not been elucidated. In this study, we intended to clarify the effect of tyloxapol on RANKL-stimulated osteoclastogenesis and the molecular mechanism both ex vivo and in vivo.

Methods: In vitro osteoclastogenesis assay was performed in BMMs and Raw 264.7 cells. The mature osteoclasts were visualized by TRAP staining. The osteoblsats were visualized by alkaline phosphatase (ALP) staining and Von Kossa staining. To assess whether tyloxapol inhibited the function of mature osteoclasts, F-actin belts and pit formation assays were carried out in BMMs. To evaluate the effect of tyloxapol on post-menopausal osteoporosis, the OVX mouse model were utilized. The bone tissue TRAP staining was used to evaluate the osteoclast activity in vivo. The von kossa staining and micro computed tomography were used to evaluate the histomorphometric parameters. The Goldner's staining was used to evaluate the osteoblast activity. The expression of osteoclastogenesis-associated markers were evaluated by Real-time PCR. The NF-κB and NFATc1 transcriptional activities were illustrated utilizing the assay of luciferase reporter. The effect of tyloxapol pretreatment on IκBa degradation and p65 phosphorylation was evaluated using Western bloting assay. The effect of tyloxapol pretreatment on p65 nuclear translocation was evaluated utilizing immunofluorescence. The effect of tyloxapol pretreatment on the phosphorylatio of ERK, p38 and JNK was examined utilizing Western bloting assay.

Results: In our research, we found that tyloxapol suppresses RANKL-stimulated osteoclastogenesis in a dose dependent manner and in the initial stage of osteoclastogenesis. Through F-actin belts and pit formation assays, we found that tyloxapol had the ability to inhibit the function of mature osteoclasts in vitro. The results of animal experiments demonstrated that tyloxapol inhibits OVX-induced bone mass loss by inhibiting the activity of osteoclasts but had a limited effect on osteoblastic differentiation and mineralization. Molecularly, we found that tyloxapol suppresses RANKL-stimulated NF-κB activation through suppressing degradation of IκBα, phosphorylation and nuclear translocation of p65. At last, MAPK signaling pathway was also suppressed by tyloxapol in dose and time-dependent manners.

* Corresponding author. Department of Orthopaedics, The Second Affiliated Hospital of Soochow University, 1055 Sanxiang Road, 215004, Suzhou, China.
** Corresponding author. Orthopaedic Oncology Center, Department of Orthopaedics, Changzheng Hospital, Second Military Medical University, Fengyang Rd 415#, Huangpu District, 200000, Shanghai, China.
*** Corresponding author. Orthopaedic Oncology Center, Department of Orthopaedics, Changzheng Hospital, Second Military Medical University, Fengyang Rd 415#, Huangpu District, 200000, Shanghai, China.
**** Corresponding author. Orthopaedic Oncology Center, Department of Orthopaedics, Changzheng Hospital, Second Military Medical University, Fengyang Rd 415#, Huangpu District, 200000, Shanghai, China.
E-mail addresses: qian_ming_qm@163.com (M. Qian), wei_haifeng@163.com (H. Wei), xiao_jianru@163.com (J. Xiao), xuyoujia@suda.edu.cn (Y. Xu).
[1] These authors contributed equally to this work.

https://doi.org/10.1016/j.jot.2021.01.005
Received 27 August 2020; Received in revised form 23 January 2021; Accepted 27 January 2021

2214-031X/© 2021 The Authors. Published by Elsevier (Singapore) Pte Ltd on behalf of Chinese Speaking Orthopaedic Society. This is an open access article under the CC BY-NC-ND license (http://creativecommons.org/licenses/by-nc-nd/4.0/).

Conclusion: Our research illustrated that tyloxapol was able to suppress osteoclastogenesis in vitro and ovariectomized-induced bone loss in vivo by restraining NF-κB and MAPK activation. This is pioneer research could pave the way for the development of tyloxapol as a potential therapeutic treatment for osteoporosis.
The translational potential of this article: This study explores that tyloxapol, also known as Triton WR-1339, may be a drug candidate for osteoclastogenic sicknesses like osteoporosis. Our study may also extend the clinical therapeutic spectrum of tyloxapol.

1. Introduction

Osteoporosis is a prevalent osteometabolic disease characterized by bony pain, microarchitectural abnormality and increased vulnerability mainly due to decreased bone mass [1–3]. Although estrogen, bisphosphonate and denosumab are reported to be effective for osteoporosis, associated adverse effects such as thromboembolism [4], esophageal irritation [5] and jaw necrosis [6,7], limit their extensive clinical applications. It is therefore necessary to develop safer and more effective drugs for it. Knowing that imbalance of bone remodeling, especially excessive enhancement of osteoclast activity, is the primary cause for osteoporosis, suppressing the abnormal bone resorption ability of osteoclasts should be an important treatment strategy.

Osteoclasts, which possess the ability of bone resorption, are formed from precursor cells belonging to the mononuclear macrophage lineage [8–10]. Osteoclasts play many critical physiological functions during bony growth and development. Many cytokines are known to be involved in the process of osteoclast maturation [9,11,12]. Macrophage colony stimulating factor (M-CSF) is one of the key regulators in mediating osteoclast proliferation and promoting the constitutive expression of RANK on the cell surface [11]. Nuclear factor kappa-B (NF-κB) ligand (RANKL) is a member of the tumor necrosis factor (TNF) family, which induces osteoclast precursors to undergo osteoclastic differentiation [13]. Under physiological conditions, the extracellular RANKL binds to its ligand RANK on the cell membrane, leading to a cascade reaction, which eventually activates NF-κB and mitogen-activated protein kinase (MAPK). During this process, osteoclastogenesis-associated marker genes such as MMP-9, NFATc1, TRAP and cathepsin K are activated, which drives osteoclastogenesis and bone resorption [14]. NF-κB activation causes degradation of IκBα, leading to p65 phosphorylation, a subunit of NF-κB, which enables NF-κB to acquire the ability of nuclear translocation to transmit information [14]. ERK, JNK and p38 belong to the MAPK family [15]. ERK enhances the expression of c-Jun and NFATc-1 induces osteoclast differentiation, which is believed to be the principal factor that brings about the occurrence of osteoclasts [15,16]. Therefore, targeting MAPK and NF-κB signaling pathway regulation is considered an approach for the treatment of osteoclast-related diseases.

Tyloxapol, also known as Triton WR-1339, is a non-ionic surfactant of alkyl aryl polyether alcohol polymer group which is widely used in biomedical applications [17,18]. On account of its brilliant surfactant properties, tyloxapol is widely utilized in numerous commercial pharmaceuticals [17–19]. Tyloxapol is reported to possess diverse pharmacological activities including the anti-inflammatory, anti-cancer and antioxidant properties [17–19]. Some studies [18] reported that tyloxapol exerted its representative pharmacological antioxidant effect by inhibiting NF-κB, which is known as a fundamental pathway for RANKL-induced formation and the function of osteoclasts. Inspired by this finding, we hypothesized that tyloxapol might have a suppressive effect on osteoclastogenesis. The aim of the present study was to explore the effect of tyloxapol on RANKL-stimulated osteoclastogenesis ex vivo, ovariectomized (OVX)-induced bone loss in vivo, and its underlying action mechanism at the molecular level.

2. Materials and methods

2.1. Reagents

Tyloxapol (purity 98.0%, CAS 25301-02-4, Targetmol, USA) (Fig. 1A) was dissolved in DMSO (dimethyl sulfoxide) and stored at −20 °C away from direct light. The DMSO, Tris, SDS, NaCl and TRAP staining kits were obtained from Sigma (St. Louis, MO, USA). Recombinant mouse M-CSF was obtained from Abcam (Cambridge, MA, USA). Alpha-MEM, penicillin, streptomycin and fetal bovine serum (FBS) were purchased from Invitrogen (Waltham, MA). Mouse RANKL was purchased from R&D System (Minneapolis, MN). The TRAP ELISA Kit was obtained from the Cloud-Clone Corp (TX, USA). Antibodies utilized in our research were obtained from Cell Signaling Technology (MA, USA).

2.2. Animals and ethics

All animals were raised, utilized and handled in our research in compliance with the rules and regulations recognized by the Ethics Committee of Soochow University (Suzhou, China). We did our utmost efforts to diminish the number of animals that were examined and their suffering. Female C57/BL6 mice aged 8 weeks (Shanghai Academy of Sciences, Shanghai, China) were utilized to extract bone marrow mononuclear cells (BMMs) and set up the OVX mouse model.

2.3. Cell culture and differentiation

In vitro osteoclastogenesis assay was performed in BMMs gathered from the whole bone marrow of the 8-week-old female C57/BL6 mice. Briefly, BMMs were grown in alpha-MEM medium containing 10 ng/mL M-CSF for 16 h, suspended, and cultured in another dish for 3 days. Finally, adherent cells on the dish were regarded as osteoclast precursor cells and utilized for osteoclastogenesis assays and grown in osteoclast differentiation medium (alpha-MEM+50 ng/ml RANKL+10 ng/ml M-CSF) for 7 days to differentiate into mature osteoclasts.

Raw 264.7 cells were grown in osteoclast differentiation medium (alpha-MEM+50 ng/ml RANKL) to generate osteoclast-like cells. After differentiation, multinucleated cells were visualized using the TRAP staining kit (Sigma, USA) according to the recommended procedures. TRAP-positive multinucleated cells (MNCs) with nuclei ≥ 3 were regarded as mature osteoclasts.

In vitro osteoblastogenesis assay was performed as follows. Bone marrow stromal cells (BMSCs) were harvested from the whole marrow cavity of 8-week-old female C57/BL6 mice, and seeded to 24-well plates at a density of $1x10^5$ cells per well. Three repeated holes were designed for each group. Osteoblast differentiation media (containing 50 mg/mL vitamin C, 10^{-8} M hexadecadrol and 10 mM β-glycerophosphate) with different concentrations of tyloxapol were used for BMSC culture. After 7-day differentiation, alkaline phosphatase (ALP) staining was performed as per provided instructions [20]. After 14-day differentiation, 2.5% silver nitrate staining solution was used to implement the Von Kossa staining.

2.4. Cytotoxicity assay

Raw 264.7, BMMs and BMSCs cells were pretreated separately with the indicated concentrations of tyloxapol for 48 h. Then, the cellular viability was evaluated utilizing the commercial MTS kit (Promega, Australia) on the basis of the manufacturer's operating instructions.

2.5. Actin belts and pit formation assay

BMMs were treated in the osteoclast differentiation medium (alpha-MEM+50 ng/ml RANKL+10 ng/ml M-CSF) and indicated concentrations of tyloxapol for 7 days, fixed in 4% PFA for 10 min, permeabilized in 0.1% Triton X-100 for 1 min, and cultured in rhodamine phalloidin (Invitrogen, USA) for 3 h to visualize the cytoskeleton of osteoclasts. Finally, they were incubated in DAPI for 10 min to visualize the nucleus.

The effect of tyloxapol on the bone erosion activity of mature osteoclasts was evaluated in vitro by pit formation assay as described previously [21,22]. Specifically, osteoclast precursor cells were laid into 96-well plates containing dentin slices ($5x10^3$ cells per well) and treated with osteoclast differentiation medium for 6 days. After multinucleated cells were observed, the culture was continued for another 2 days. Thereafter, the dentin slices were fixed with 4% PFA for more than 10 min. After that, 1 N NH4OH was utilized for 5 min to burst the osteoclasts. Finally, 0.5% toluidine blue was utilized for 5 min to colorize the resorption pits on the dentin slices. The resorption pits were visualized by light microscopy and confocal microscopy.

2.6. Immunofluorescence of p65

The effect of tyloxapol on p65 nuclear translocation was observed by immunofluoresistation. After 30-min stimulation using osteoclast differentiation medium with or without tyloxapol, raw 264.7 cells were immersed in the solution containing anti-p65 antibody for 3 h, and incubated with Alexa Fluor® conjugated secondary antibody (abcam) for 15 min. Finally, DAPI was used to incubate the cells for 10 min to visualize the nucleus. Immunofluorescence images were obtained under a confocal microscope.

2.7. Luciferase reporter assays

To observe the inhibitory effect of tyloxapol on the NF-κB and NFATc1 activities, luciferase reporter assays were carried out. Specifically, RAW264.7 cells were co-transfected with 0.45 μg of the reporter plasmids pGL4.32[luc2P/NF-kB-RE/Hygro] or pGL4.30[luc2P-NFAT-RE-Hygro], and 0.05 μg of null Renilla vector (Promega Madison, WI, USA), as an internal control, using the FuGene HD method (Roche Applied Sciences, Penzberg, Germany) in accordance with the manufacturer's instructions. 48 h later, RAW264.7 cells were exposed to the indicated concentrations of tyloxapol for 2 h, followed by 50 ng/ml RANKL for 12 h. The luciferase activities were quantified utilizing the promega dual-Luciferase® reporter assay kit following the recommended protocol.

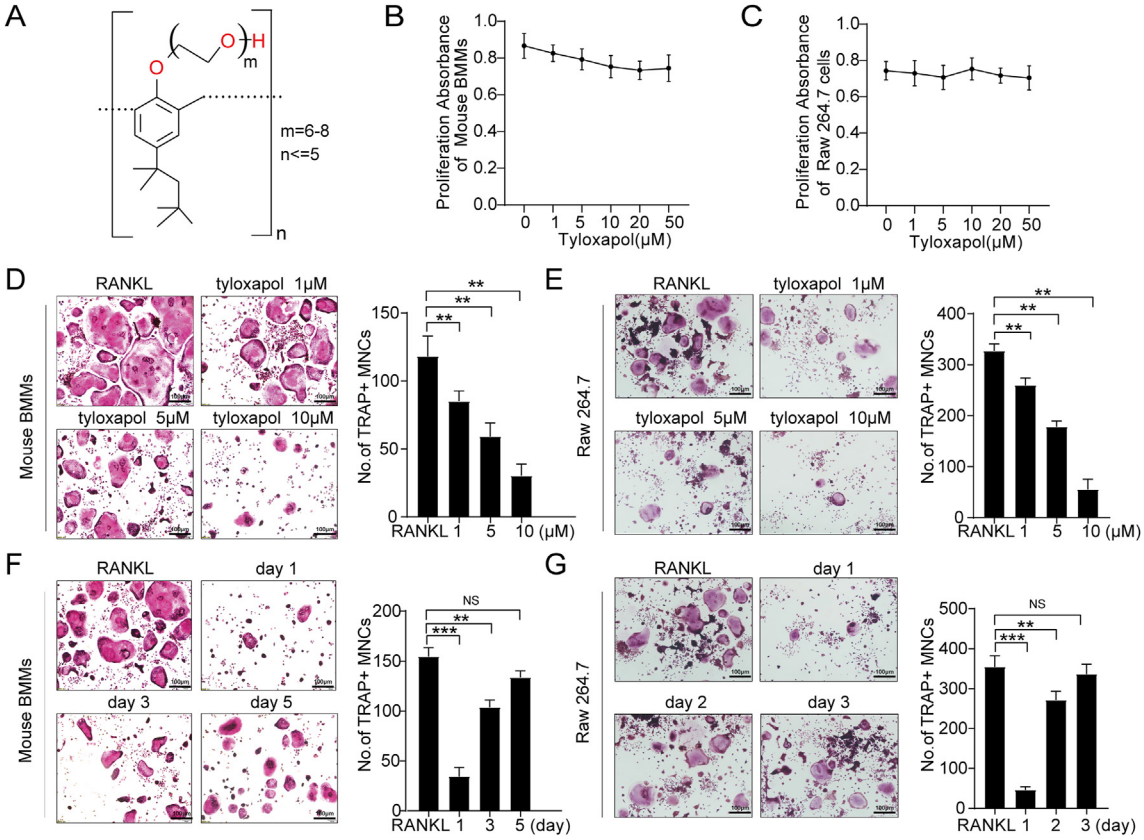

Figure 1. Tyloxapol suppressed osteoclastogenesis in BMMs and RAW264.7 cells. (A) Molecular structure of tyloxapol. (B, C) The cell viability of BMMs and Raw 264.7cells after pretreatment with indicated concentrations of tyloxapol for 48 hours examined by MTS. (D, E) Tyloxapol suppressed osteoclastogenesis in BMMs and Raw 264.7 in a dose-dependent manner. Mouse BMMs ($8x10^3$ cells) or RAW264.7 cells ($3x10^3$ cells) were cultured in alpha-MEM containing 50 ng / mL RANKL with or without 10 ng / mL M-CSF. The indicated doses of tyloxapol were utilized to pretreated these cells for 7 days or 5 days. The cells were stained using TRAP staining kit. TRAP-positive MNCs with more than 5 nucleis were counted. (F, G) Tyloxapol suppressed osteoclastogenesis in BMMs and Raw 264.7 at the early stage of osteoclastogenesis. The indicated doses of tyloxapol were utilized at the indicated days during the progress of osteoclastogenesis in BMMs. The cells were stained using TRAP staining kit. TRAP-positive MNCs with more than 5 nucleis were counted. Columns in the charts were presented in a manner of mean ± SD, n=3. Scale bars=100 μm. *P < 0.05, **P < 0.01, ***P < 0.001, unpaired two-tailed Student's t test. MNCs=multinucleated cells.

2.8. Real-time PCR (RT-PCR)

BMMs were pretreated with gradient concentrations of tyloxapol for 5 days followed by 50 ng/ml RANKL with or without tyloxapol for 12 h. Total RNA was extracted utilizing TRIzol Reagent (Invitrogen, Carlsbad CA, USA) in accordance with the manufacturer's protocol. cDNA was synthesized from 1 μg of extracted RNA utilizing reverse transcriptase (TaKaRa Biotechnology, Otsu, Japan). RT-PCR was carried out utilizing the SYBR Premix Ex Taq Kit (Takara Biotechnology) and amplified by the ABI Prism 7500 System (Thermo Fisher Scientific) in conformity with the equipment operation manual. All samples were assessed in triplicate, using β-actin for normalization. The following primers were used in our experiments:

β-actin: Forward primer: CTCCCACTCTTCCACCTTCG, Reverse primer: TTGCTGTAGCCGTATTCATT;

TRAP: Forward primer: GCTGGAAACCATGATCACCT, Reverse primer: GAGTTGCCACACAGCATCAC;

CathepsinK: Forward primer: CTTCCAATACGTGCAGCAGA, Reverse primer: TCGGTTTCTTCTCCTCTGGA;

MMP9: Forward primer: ACCCTTGTGCTCTTCCCTG, Reverse primer: GGCAAGTCTTCCGAGTAGTTT;

NFATc1: Forward primer: TGGAGAAGCAGAGCACAGAC, Reverse primer: GCGGAAAGGTGGTATCTCAA;

Bsp: Forward primer: TTTGGGAATGGCCTGTGCTTTCTC; Reverse primer: AGTGTGGAAAGTGTGGAGTTCTCTGC;

Ocn: Forward primer: AGTCACCAACCACAGCATCC, Reverse primer: TTTGTCCCTTCCCTTCTGCC.

2.9. Western blotting analysis

Pre-treated cells were gathered on ice and lysed with RIPA lysis buffer. Proteins of different molecular weights were then separated using 10% SDS-PAGE at the voltage of 80 or 120 V. The isolated protein was then transferred to the NC membrane using electroporation. Non-specific proteins on the NC membrane were blocked with PBST solution containing 5% bovine serum protein or skimmed milk powder for 60 min. The NC membranes were then immersed sequentially with primary antibodies and the secondary antibodies at 4 °C or 37 °C for 14 h or 1 h. The expression of specific proteins were visualized employing the Odyssey Infrared Imaging System (LI-COR Bioscience, Lincoln, NE, United States).

2.10. OVX induced osteoporosis model

Following the methodology used in classical research [22], we set up an OVX mouse model to assess the effect of tyloxapol on bone loss in vivo. One week after ovariectomy, 8-week-old female C57BL/6 mice were equally randomized into three groups: sham operation (SHAM) group, vehicle (OVX) group, and tyloxapol-treated (OVX + Tyloxapol) group. Tyloxapol (200 mg/kg) or DMSO (1% in normal saline) was injected intraperitoneally (i.p.) into mice every other day. Twelve weeks after drug injection, the experimental mice were anesthetized by an overdose of avertin. The distal femur bone tissue was de-calcified, paraffin embedded, sliced into sections and TRAP stained to determine whether the osteoclast activity was affected. The third lumbar vertebra was washed, embedded in polymethylmethacrylate, sliced into sections, and von kossa stained to determine whether the bone mass was affected, and Goldner's stained [23] to determine whether the osteoblast activity was affected. The histomorphometric parameters of the distal femoral metaphysic were evaluated by micro computed tomography (μCT). TRAP level in mouse serum was detected using the mouse TRAP ELISA kit (Cloud--Clone Corp, Houston, USA).

At 3 weeks after ovariectomy, three groups (SHAM, OVX, Tyloxapol) of mice received intraperitoneal injection of 30 mg/kg calcein on day 0 and day 7. Mice were sacrificed on day 10, and the isolated third lumbar vertebra were dehydrated and embedded in polymethylmethacrylate. The vertebras were cut into 4 μm sections to capture the fluorescence-labelled images. The mineral apposition rate (MAR) and bone formation rate per bone surface (BFR/BS) were measured to determine whether the bone formation activity was affected by tyloxapol.

2.11. Statistical analysis

GraphPad Prism 8.0.1 (GraphPad Software, LLC.) was utilized for the statistical analysis. The mean ± standard deviation was recorded for all the experiments. Statistical significance between two groups was assessed with Student' s t-test, and multiple comparisons were performed using one-way analysis of variance (ANOVA). Triplicate experimental repeats were conducted. P values < 0.05 were regard to be statistically significant.

3. Results

3.1. Tyloxapol suppresses RANKL-stimulated osteoclastogenesis in the early phase

To illustrate the effect of tyloxapol on osteoclastogenesis, two standardized osteoclast differentiation models (BMMs and Raw 264.7) were utilized [24]. As shown in Fig. 1D and E, the higher the concentration of tyloxapol, the fewer TRAP-positive MNCs were observed, indicating that tyloxapol inhibited the osteoclastogenesis in a dose dependent manner. The process of osteoclastogenesis usually undergoes four processes: proliferation, differentiation, cell fusion, and multinucleation. To clarify the specific phase in which tyloxapol started to impede osteoclast differentiation, tyloxapol was added to the osteoclast differentiation medium at the indicated time points. The results illustrated that addition of tyloxapol in the initial stage of differentiation could maximally suppress osteoclast formation, while the inhibitory effect of tyloxapol addition in a later stage was feeble (Fig. 1F and G). All these results showed that tyloxapol suppressed RANKL-stimulated osteoclastic differentiation in the early phase of osteoclastogenesis. To rule out the hypothesis that cytotoxicity of tyloxapol could suppress osteoclastogenesis, we further examined its cytotoxicity to BMMs and RAW264.7 through MTS experiments. As shown by the MTS results (Fig. 1B and C), the anti-osteoclastogenic activity of tyloxapol was not related to its toxicity and the one-half maximal inhibitory concentration (IC50) was >50 μM in BMMs and RAW264.7 cells.

3.2. Tyloxapol suppresses the function of mature osteoclasts in vitro

To further assess whether tyloxapol inhibited the function of mature osteoclasts, F-actin belts and pit formation assays were carried out utilizing the BMMs osteoclast differentiation model. The actin belts assay was carried out first, showing that BMMs differentiated into mature osteoclasts under the action of differentiation medium (Fig. 2A and B). After tyloxapol intervention, a significant decrease in the area and number of the actin belts was observed. Second, pit formation assay showed that many large and deep absorption pits were generated in SHAM group under the stimulation of RANKL (Fig. 2D and E). However, the depth and area of bone pits on bone slices were decreased significantly upon 10 mM tyloxapol intervention. The above two experiments showed that tyloxapol had the ability to inhibit the function of mature osteoclasts in vitro.

3.3. Tyloxapol inhibits OVX-induced bone mass loss by inhibiting the activity of osteoclasts in mice

Over-activation of osteoclasts is one of the principal pathogeneses of osteoporosis. Estrogen insufficiency can boost osteoclast manufacture and activity, and is a significant factor in bringing about menopausal osteoporosis [25]. To evaluate the effect of tyloxapol on post-menopausal osteoporosis, we utilized the OVX mouse model to simulate this

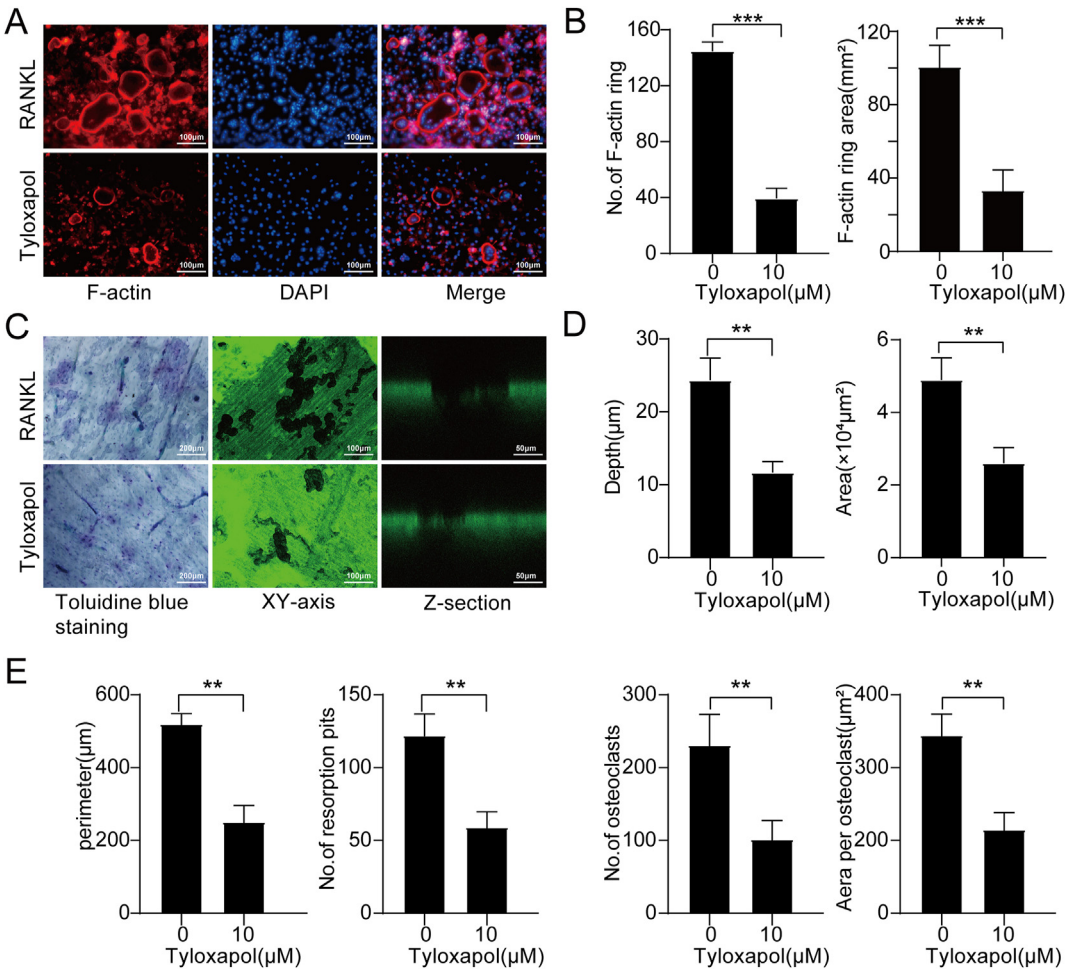

Figure 2. Tyloxapol suppressed the function of mature osteoclasts in vitro. (A, B) Representative F-actin belts images of mouse BMMs pretreated with or without tyloxapol. Mouse BMMs ($5x10^3$ cells) were cultured in alpha-MEM containing 10 ng/mL M-CSF and 50 ng /mL RANKL pretreated with or without tyloxapol for 7 days, and then the F-actin belts staining was performed as mentioned in the materials and methods (Fig. 2A). The number and area of F-actin belts per well was counted (Fig. 2B). Columns in the charts were presented in a manner of mean ± SD, n=3. Scale bars=100 μm. (C, D, E) Representative dentine slices images of mouse BMMs pretreated with or without tyloxapol were taken using light microscopy and confocal microscopy. Mouse BMMs ($5x10^3$ cells) were cultured in alpha-MEM containing 10 ng/mL M-CSF and 50 ng /mL RANKL pretreated with or without tyloxapol for 8 days, and then the dentine slices staining was performed as mentioned in the materials and methods. The depth, area, perimeter, No. of resorption pits scanned, No. of osteoclasts and area per osteoclast scanned by confocal microscopy (xy section and z section) were calculated. Columns in the charts were presented in a manner of mean ± SD. n=3. Scale bars: 200 μm for the toluidine blue staining, 100 μm for the xy-axis and 50 μm for the Z-section.

pathophysiological phenomenon. Bone parameter analysis from the results of von kossa and the micro CT showed that the bone volume per tissue volume (BV/TV), trabecular separation (Tb.Sp), and trabecular number (Tb.N), osteoclast surface/bone surface area (OcS/BS) and eroded surface/bone surface (ES/BS) of OVX group were decreased as compared with SHAM group, and the levels of these indicators reversed to some extent after treated by tyloxapol for 12 weeks (Fig. 3A and B). The effect of tyloxapol on the osteoclast activity in OVX mice were also assessed by immunohistochemical TRAP staining of the femur (Fig. 3C and D) and ELISA assay for the serum (Fig. 3B). The results of animal experiments demonstrated that administration of 200 mg/kg tyloxapol in OVX group impaired osteoclast activity to some extent.

3.4. Tyloxapol does not effectively enhance osteoblast differentiation

The effect of tyloxapol on osteoblast differentiation was also examined in this study. To rule out the toxic effect of tyloxapol on osteoblasts, we carried out an MTS cell proliferation assay. As shown in Fig. 4H, the effect of tyloxapol on osteoblasts at a concentration that could effectively inhibit osteoclast differentiation did not show significant toxicity. The results of ALP staining and von Kossa staining (Fig. 4A and B) showed that tyloxapol had a limited effect on osteoblastic differentiation and mineralization. The effect of tyloxapol on the osteoblast activity in OVX mice was evaluated by Goldner's trichrome staining in the lumbar vertebrae (Fig. 4C and D). Unsurprisingly, the results are consistent with those in vitro. The results of Calcein double labelling assay (Fig. 4E) showed that tyloxapol had a limited effect on the bone formation activity. In addition, after tyloxapol treatment, the expression of the osteoblastic differentiation-associated marker genes Bsp and Ocn) was comparable to that in SHAM group (Fig. 4F). In summary, tyloxapol did not show any significant effect to osteoblast differentiation ex vivo and in vivo.

3.5. Tyloxapol suppresses RANKL-stimulated NF-κB activation through suppressing degradation of IκBα

Knowing that NF-κB is a critical pathway during osteoclastogenesis, we firstly checked whether tyloxapol had any impact on this pathway. Three kinds of assay were performed to address this question. Firstly, the NF-κB transcriptional activity was illustrated utilizing the assay of luciferase reporter. As shown in Fig. 5B, the NF-κB transcriptional activity was increased significantly after RANKL stimulation. However, tyloxapol inhibited this tendency in a dose-dependent manner (Fig. 5B).

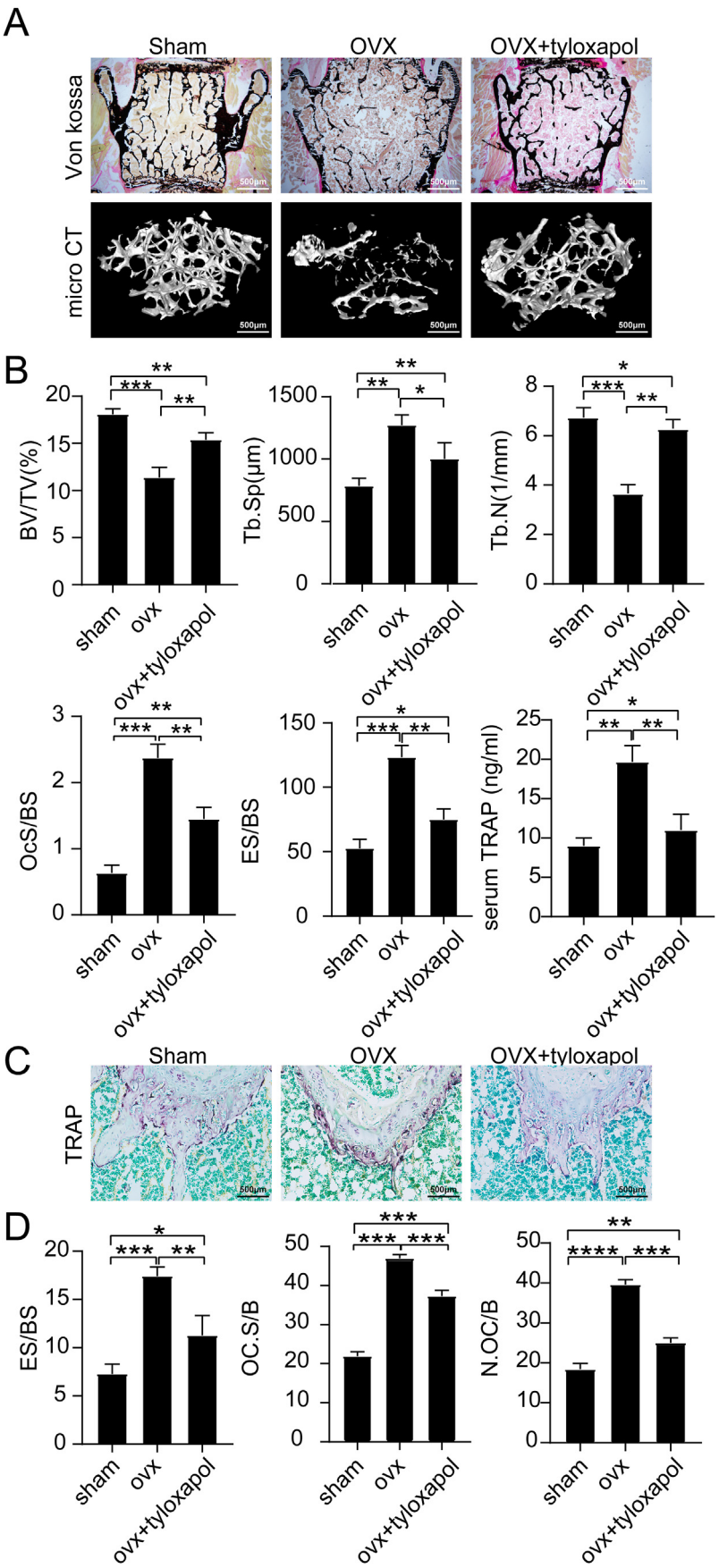

Figure 3. Tyloxapol inhibited OVX-induced bone mass loss by suppressing osteoclast activity and function in mice. (A) Representative images of von kossa-staining of L3 vertebrae and μCT of the femur from mice groups of sham, OVX, and OVX+tyloxapol. Scale bars=500μm. (B) Bone parameter analysis from the results of von kossa and the micro CT containing the bone volume per tissue volume (BV/TV), trabecular separation (Tb.Sp), and trabecular number (Tb.N), osteoclast surface/bone surface area (OcS/BS) and eroded surface/bone surface (ES/BS). Serum TRAP activity was measured by ELISA assay. Column, means of three experiments performed in triplicate; bar, SD. (C) Representative images of TRAP-staining of femur. Scale bars=500μm. (D) Bone parameter analysis from the results of TRAP-staining of femur containing the number of osteoclasts/ bone perimeter (N.Oc/B),the eroded surface/bone surface (ES/BS) and the osteoclast surface/bone surface (Oc.S/BS). Columns in the charts were presented in a manner of mean ± SD. n=6. *P < 0.05, **P < 0.01, ***P < 0.001, unpaired two-tailed Student's t test.

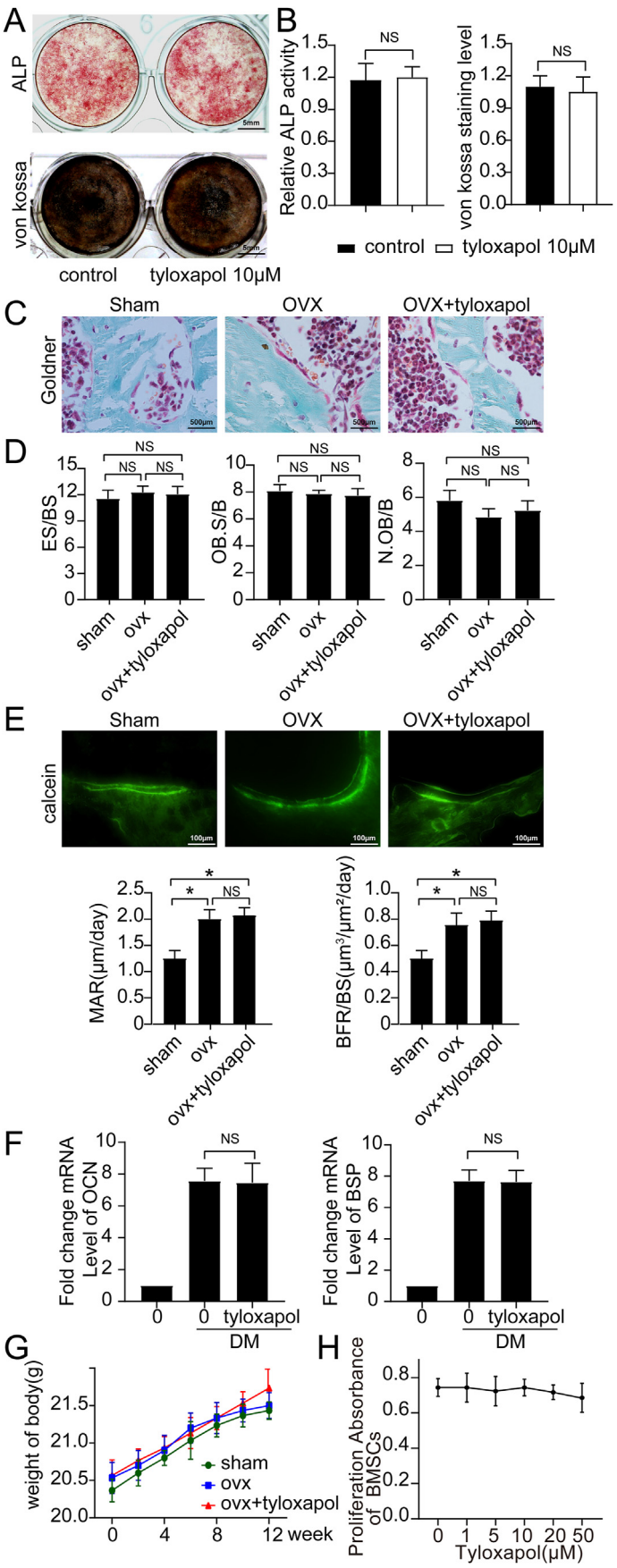

Figure 4. Tyloxapol could not effectively enhance osteoblast differentiation in vitro and vivo. (A, B) Representative images of the ALP and von kossa staining of BMSCs pretreated with or without tyloxapol. BMSCs with a density of $1x10^5$ cells/well were added to 24-well plates and cultured as mentioned in the materials and methods. The ALP activity and von kossa staining levels were counted. Columns in the charts were presented in a manner of mean ± SD. n=3. Scale bars, 5mm. (C) Representative Goldner's trichrome-staining of L3 vertebrae of sham, OVX, and OVX+tyloxapol mice. Scale bars, 500μm. (D) Histomorphometric analysis from the results of Goldner's trichrome-staining containing eroded surface/bone surface (ES/BS), osteoblast surface per bone surface (OB.S/B) and osteoblast number per bone perimeter (N.OB/B). Columns in the charts were presented in a manner of mean ± SD. n=6. (E) Representative Calcein double labelling of L3 vertebrae of sham, OVX, and OVX+tyloxapol mice. Scale bars, 100μm. Histomorphometric analysis from the results of Calcein double labelling containing mineral apposition rate (MAR) and bone formation rate per bone surface (BFR/BS). Columns in the charts were presented in a manner of mean ± SD. n=6. (F) Tyloxapol had little effect on osteoblast marker genes expression including OCN and BSP analyzed by real-time PCR. Columns in the charts were presented in a manner of mean ± SD. n=3. (G) Trends of body weight of mice in each experimental groups within 12 weeks. No statistically significant difference was found between these trends of body weight. n=6, mean ± SD. (H) The cell viability of BMSCs after pretreatment with indicated concentrations of tyloxapol for 48 hours examined by MTS. mean ± SD. n=3. NS=not significant, unpaired two-tailed Student's t test. DM=osteoblast differentiation medium. BMSCs=Bone marrow stromal cells.

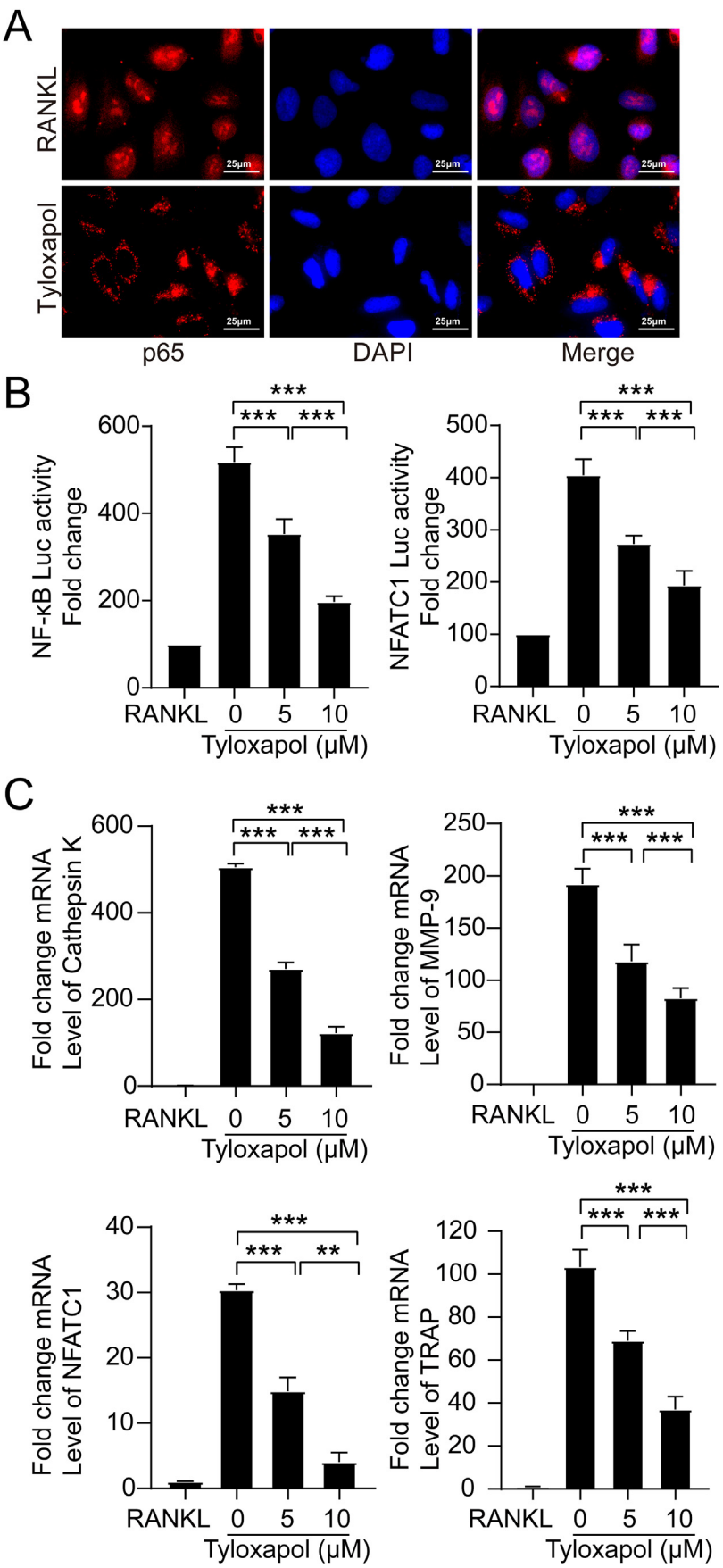

Figure 5. Tyloxapol suppressed RANKL-stimulated NF-κB activation and osteoclastogenesis-related gene expression.(A)Representative immunofluorescence images of the translocation of p65. Tyloxapol suppressed RANKL-stimulated p65 translocation. Scale bars, 25μm. (B) The luciferase activity of p65 and NFATc1 were measured utilizing the luciferase reporter assay. Tyloxapol suppressed RANKL-stimulated transcriptional activity increase of the p65 and NFATc1 in a dose-dependent manner. (C) The mRNA levels of cathepsin K, MMP-9, NFATc1 and TRAP of Raw 264.7 cells pretreated with or without tyloxapol. Tyloxapol suppressed RANKL-stimulated mRNA expression levels increase of these genes in a dose-dependent manner. Columns in the charts were presented in a manner of mean ± SD. n=3. *P < 0.05, **P < 0.01, ***P < 0.001, unpaired two-tailed Student's t test.

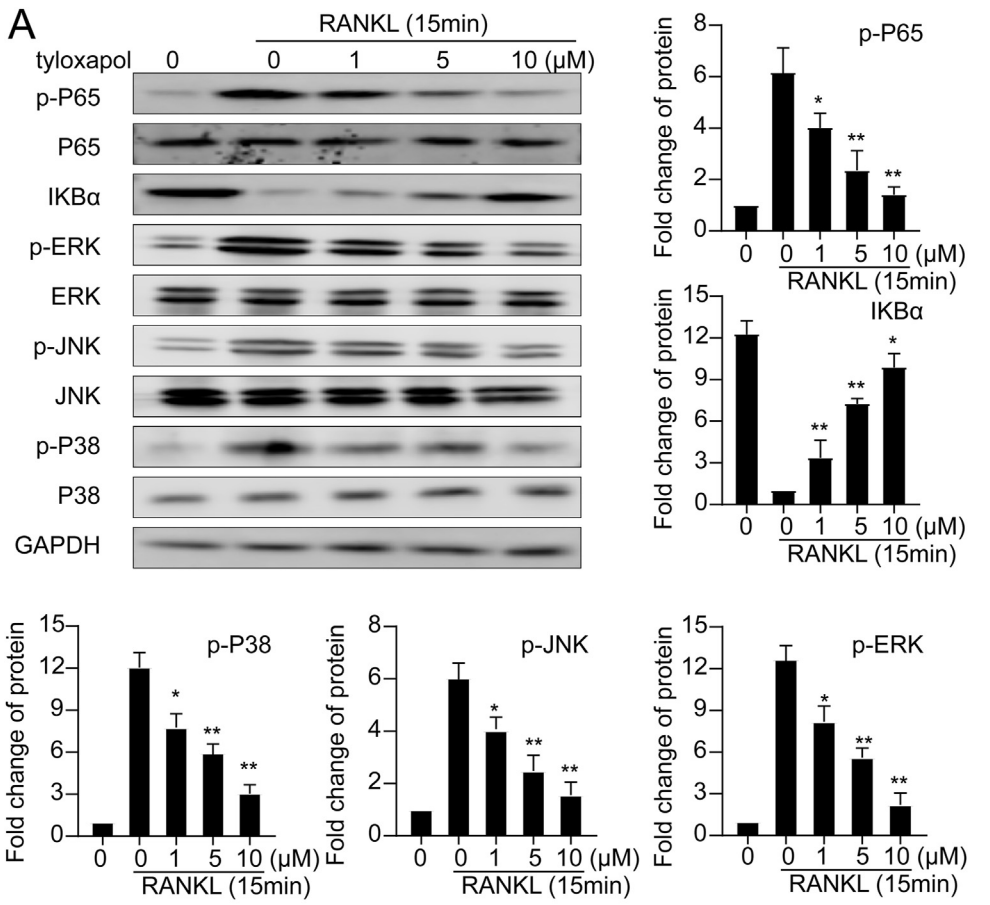

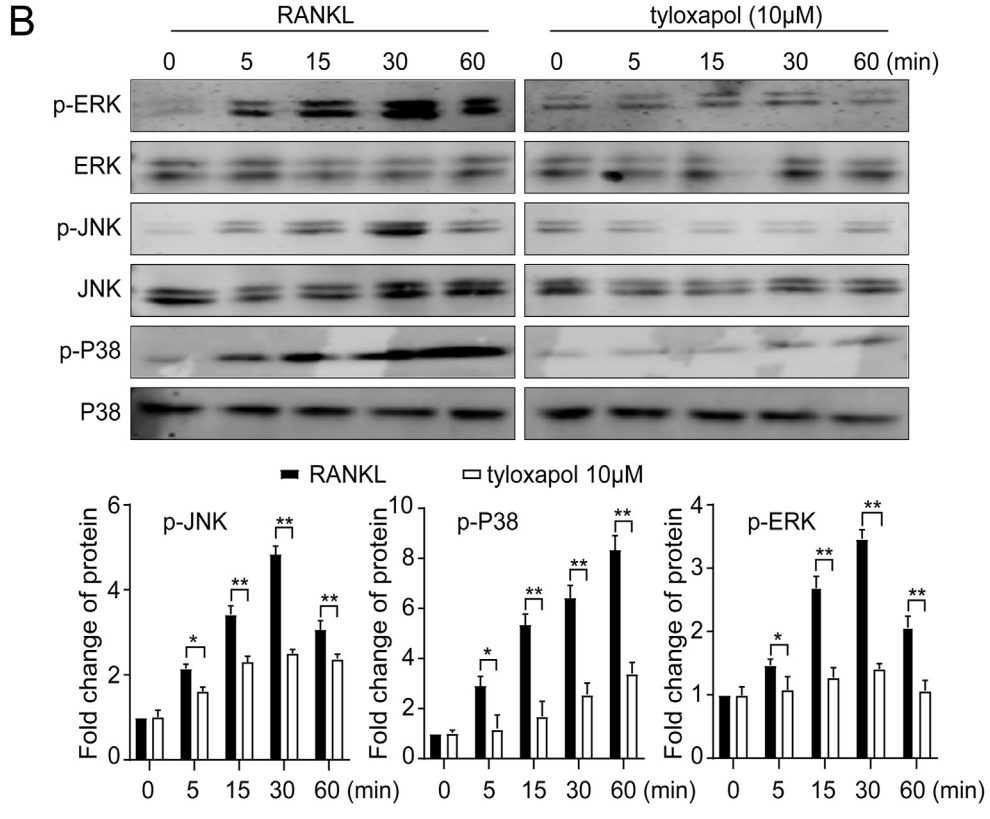

Figure 6. Tyloxapol suppressed RANKL-stimulated NF-κB and MAPKs activation. (A) The protein expression levels of p-p65, p65, IκBα, p-ERK, ERK, p-JNK, JNK, p-p38 and p38 were examined utilizing the western blot assays for Raw 264.7 cells pretreated with tyloxapol at indicated concentrations. Tyloxapol dose-dependently inhibited RANKL-stimulated degradation of IκBα and phosphorylation of p65, ERK, JNK and p38. All bar charts are presented as mean ± SD; n=3. *P < 0.05, **P < 0.01 vs group only treated with RANKL. (B) The protein expression levels of p-ERK, ERK, p-JNK, JNK, p-p38 and p38 were examined utilizing the western blot assays for Raw 264.7 cells pretreated with tyloxapol at indicated times. Tyloxapol time-dependently suppressed RANKL-stimulated phosphorylation of ERK, JNK and p38. All bar charts are presented as mean ± SD; n=3. *P < 0.05, **P < 0.01, ***P < 0.001, unpaired two-tailed Student's t test.

Secondly, the effect of tyloxapol treatment on IκBa degradation and p65 phosphorylation was evaluated using Western bloting assay. The results showed that tyloxapol pretreatment inhibited RANKL-induced IκBa degradation in a dose-dependent manner (Fig. 6A). Thirdly, the effect of tyloxapol treatment on p65 nuclear translocation was evaluated utilizing immunofluorescence. As shown in Fig. 5A, the p65 nuclear translocation was increased significantly after RANKL pretreatment. However, the increase of p65 nuclear translocation decreased significantly when RANKL pretreatment was conducted in the presence of tyloxapol (Fig. 5A).

3.6. Tyloxapol suppresses RANKL-stimulated NFATc1 activation

NFATc1 is also a critical transcription factor during osteoclastogenesis, so we evaluated the effect of tyloxapol on NFATc1 activation using luciferase reporter assay and RT-PCR in RAW 264.7 cells. As seen from the Fig. 5B and C, RANKL stimulation increased the NFATc1 transcriptional activity and the mRNA expression level significantly. However, tyloxapol inhibited this effect in a dose-dependent manner (Fig. 5B and C).

3.7. Tyloxapol suppresses RANKL-stimulated MAPK activation

MAPK is another critical signaling pathway contributing to osteoclastogenesis. The effect of tyloxapol pretreatment on the phosphorylatio of ERK, p38 and JNK was examined utilizing Western bloting assay. As shown in Fig. 6A and B, the ERK, p38 and JNK phosphorylation level was increased significantly after RANKL pretreatment, but this effect could be reversed by tyloxapol in dose and time-dependent manners.

3.8. Tyloxapol suppresses the expression of osteoclastogenesis-associated markers

The expressions of many maker genes, such as MMP-9, cathepsin K and TRAP, are strengthened during osteoclastogenesis [26]. Fig. 5C shows that the mRNA expression levels of these maker genes were increased by several fold when stimulated with an appropriate amount of RANKL. However, the growth rate decreased after tyloxapol pretreatment.

4. Discussion

Generally, bone remodeling is a dynamic procedure controlled by the coordinated activity of osteoblasts (which produce bone) and osteoclasts (which resorb bone). Once this balance is disturbed, especially due to excessive enhancement of the osteoclast activity, a series of diseases, including osteoporosis, osteolytic bone tumors and rheumatoid arthritis may develop [2]. Therefore, the main treatment strategy for bone metabolic diseases is to suppress the over activity of osteoclasts. Further reports suggest that tyloxapol can alleviate inflammation via inhibiting NF-κB pathway [18]. However, the role of tyloxapol during osteoclastogenesis remains unknown, and the molecular mechanism remains uncertain. The aim of the present study was to examine the effect of tyloxapol on osteoclast formation and explore the underlying action mechanism ex vivo and in vivo at a molecular level. It was discovered that tyloxapol suppressed RANKL-stimulated osteoclastogenesis, F-actin belts constitution, and the osteoclast erosion ability ex vivo. Tyloxapol also restrained bone mass loss through suppressing the osteoclast activity in the mouse osteoporosis model. Eventually, we illustrated that tyloxapol inhibited the expression of osteoclastogenesis-associated maker genes NFATc1, TRAP, cathepsin K and MMP9 by attenuating the NF-κB and MAPK pathways.

In the process of osteoclastogenesis, the primary function of M-CSF is to maintain BMM proliferation and guide its differentiation to osteoclast precursors, while the main role of RANKL is to stimulate osteoclast precursors to differentiate into mature osteoclasts [26]. It was found in this study that tyloxapol had a minimal effect on the M-CSF-driven proliferation of BMMs and Raw 264.7 in a certain concentration range. However, it could inhibit RANKL-stimulated differentiation of osteoclast precursors to osteoclasts to a certain extent. These findings suggest that tyloxapol was able to exert an inhibitory effect on RANKL-stimulated osteoclastic differentiation and maturation, which indirectly proves that it inhibits RANKL signaling.

The key driver of the pathological bone destruction is the ability of osteoclasts to cause bone erosion, mainly depending on their adhesion to the mineralized bone surface [10]. Differentiated osteoclasts polarize and develop a sealing region around the bone resorption domain with F-actin belts [10]. This study showed that tyloxapol suppressed RANKL-induced F-actin loop establishment and the osteoclast erosion capability, indicating that tyloxapol can significantly inhibit RANKL-induced osteoclast erosion in vitro.

NF-κB signaling is an important essential signaling pathway for immune and inflammatory responses and is the main downstream signaling pathway for RANKL-induced osteoclast differentiation [14,27]. Typically, nuclear translocation of inactive NF-κB cannot take place until its inhibitor IκBα is degraded. Due to IKK activation, IκBα phosphorylates at ser32 and ser36 and degrades gradually when upstream signals are stimulated. Without IκBα inhibition, NF-κB undergoes nuclear translocation to transmit the signal into the nucleus [14]. We illustrated that tyloxapol restrained activation of the RANKL-stimulated NF-κB pathway, as evidenced by inhibition of IkBα degradation, blockage of phosphorylation and nuclear translocation of p65. Our experiment demonstrated that the mechanism of tyloxapol in inhibiting osteoclast differentiation may also be attributed to attenuation of the NF-κB pathway.

Other than NF-κB, MAPKs including ERK, JNK and p38 were also found to be activated in RANKL-stimulated osteoclastogenesis [15,24,28]. ERK plays an enhancement role in osteoclast survival. It was reported that p38 signaling was indispensable in early phases of osteoclast formation, for it can alleviate the expression of cathepsin K [15]. At the end of osteoclast formation, JNK was also found to participate in the fusion process of osteoclast precursors [15]. This study demonstrated that tyloxapol suppressed RANKL-stimulated phosphorylation of ERK, p38 and JNK effectively, indicating that tyloxapol can prevent the cascade of MAPK signaling pathway.

It was illustrated that the estrogen level was reduced in OVX mice, which induced osteoblasts and T cells to secrete more cytokines such as RANKL and TNFa, resulting in osteoclastogenesis and bone mass loss [29]. Bone parameter analysis from the results of von kossa, micro CT and TRAP staining illustrated that tyloxapol prevented bone loss by attenuating the osteoclast activity and osteoclast formation. Bone remodeling hinges on the dynamic balance of osteoclast bone erosion and osteoblast bone generation. Therefore, ALP and Von Kossa staining for osteoblasts in vitro and Goldner's trichrome staining in vivo were done to examine the effect of tyloxapol on osteoblast differentiation and activity. Moreover, we performed calcein double labeling analysis on the third lumbar vertebra for dynamic histomorphometry. These experiments illustrated that tyloxapol had a minimal effect on osteoblast differentiation but was able to restrain bone mass loss induced by ovariectomy through suppressing osteoclastogenesis without increasing bone establishment. Some of our experimental results are inconsistent with the classical experimental results. For example, in Fig. 4D, there is no change on osteoblast surface or osteoblast number induced by either OVX or tyloxapol in our results. But in previous reports, OVX induced higher turnover which includes higher bone resorption and higher bone formation [30–32]. There may be some reasons for this phenomenon. Firstly, although the osteoporosis model of c57 mice has been widely used, the instability of this model still exists. Iwaniec et al. [33] illustrated that little difference of BV/TV was observed between OVX and SHAM groups in the distal femur three months after the ovariectomy. Klinck and Boyd [34] demonstrated that lots of morphology parameters were not statistically significant in the C57BL/6J at 5 weeks after the ovariectomy. Therefore, the use of more models to verify the in vivo effect of tyloxapol is needed in future experiments.

There are some limitations in this study. First, we only conducted a preliminary study on the mechanism of how tyloxapol inhibited osteoclast differentiation, and future studies need to focus on more in-depth mechanisms, such as combining targets and more accurate intracellular signal transduction. In addition, the treatment status of the mice was not blinded in our study, which may lead to bias in the interpretation of the results.

5. Conclusions

This is pioneer research illustrated that tyloxapol was able to suppress osteoclastogenesis in vitro and in vivo by suppressing NF-κB and MAPK signaling, suggesting that tyloxapol may prove to be a drug candidate for osteoclastogenic sicknesses like osteoporosis. Our research may also extend the clinical therapeutic spectrum of tyloxapol.

Funding source

This work was supported by grants from the National Key Research and Development Program of China, China (2019YFC1316000), the National Natural Science Foundation of China, China (81874018), the Science and Technology Commission of Shanghai Municipality, China (20ZR1457500, 17ZR1439000), Social Development-Clinical Frontier Technology-Key Project of Jiangsu province (BE2019661), Gusu Health Talent Program (GSWS2019004), Mingsheng science and technology project of Suzhou City(SS201814).

Compliance with ethical standards

Disclosure of potential conflicts of interest

Author contributions

W.G., Y.X., J.X. designed research; W.G., H.L., Y.L. conducted the experiments and acquired data; W.G., Y.L. analysed data and performed statistical analysis; W.G. wrote the manuscript; Y.X., J.W. provided good suggestions during the study process and manuscript revising. All authors have approved the final article.

Declaration of competing interest

All authors report no conflicts of interest.

Acknowledgments

Sincere thanks to Xin Gao, Tao Wang, Bin Liu, Jian Lu, Zheyu Wu, Liang Tang, Binghua Ru, Zhixiang Wu, Liang He, Wenhao Jiang for their help of laboratory work. We thank Zhenxi Li, Youjia Xu for helping with the design of the experiment.

References

[1] Aspray TJ, Hill TR. Osteoporosis and the ageing skeleton. Subcell Biochem 2019;91:453–76.
[2] Ensrud KE, Crandall CJ. Osteoporosis. Ann Intern Med 2018;168:306–7.
[3] Russell LA. Management of difficult osteoporosis. Best Pract Res Clin Rheumatol 2018;32:835–47.
[4] Levin VA, Jiang X, Kagan R. Estrogen therapy for osteoporosis in the modern era. Osteoporos Int 2018;29:1049–55.
[5] Zebic L, Patel V. Preventing medication-related osteonecrosis of the jaw. BMJ 2019;365:l1733.
[6] Tm Y, Lee KH, Lee SH, Park W. Denosumab-related osteonecrosis of the jaw: a case report and management based on pharmacokinetics. Oral Surg Oral Med Oral Pathol Oral Radiol 2015;120:548–53.
[7] Sakaida H, Yuasa H, Fukutome K, Takeuchi K. Pharyngolaryngeal ulcers associated with the improper use of alendronate. Auris Nasus Larynx 2017;44:762–5.
[8] Miron RJ, Zohdi H, Fujioka-Kobayashi M, Bosshardt DD. Giant cells around bone biomaterials: osteoclasts or multi-nucleated giant cells. Acta Biomater 2016;46:15–28.
[9] Ono T, Nakashima T. Recent advances in osteoclast biology. Histochem Cell Biol 2018;149:325–41.
[10] Ishii M, Saeki Y. Osteoclast cell fusion: mechanisms and molecules. Mod Rheumatol 2008;18:220–7.
[11] Kong L, Wang B, Yang X, He B, Hao D, Yan L. Integrin-associated molecules and signalling cross talking in osteoclast cytoskeleton regulation. J Cell Mol Med 2020;24:3271–81.
[12] Park JH, Lee NK, Lee SY. Current understanding of RANK signaling in osteoclast differentiation and maturation. Mol Cell 2017;40:706–13.
[13] Jin H, Shao Z, Wang Q, Miao J, Bai X, Liu Q, et al. Sclareol prevents ovariectomy-induced bone loss in vivo and inhibits osteoclastogenesis in vitro via suppressing NF-κB and MAPK/ERK signaling pathways. Food Funct 2019;10:6556–67.
[14] Abu-Amer Y. NF-κB signaling and bone resorption. Osteoporos Int 2013;24:2377–86.
[15] Thouverey C, Caverzasio J. Focus on the p38 MAPK signaling pathway in bone development and maintenance. BoneKEy Rep 2015;4:711.
[16] Wang Q, Yuan X, Li B, Sun D, Liu J, Liu T, et al. Roles of SP600125 in expression of JNK, RANKL and OPG in cultured dental follicle cells. Mol Biol Rep 2019;46:3073–81.
[17] Serikov VB, Glazanova TV, Jerome EH, Fleming NW, Higashimori H, Sr SNC. Tyloxapol attenuates the pathologic effects of endotoxin in rabbits and mortality following cecal ligation and puncture in rats by blockade of endotoxin receptor-ligand interactions. Inflammation 2003;27:175–90.
[18] Ghio AJ, Marshall BC, Diaz JL, Hasegawa T, Samuelson W, Povia D, et al. Tyloxapol inhibits NF-kappa B and cytokine release, scavenges HOCI, and reduces viscosity of cystic fibrosis sputum. Am J Respir Crit Care Med 1996;154:783–8.
[19] Heck SO, Zborowski VA, Chagas PM, da Luz S, Bortolatto CF. p-Chloro-diphenyl diselenide attenuates plasma lipid profile changes and hepatotoxicity induced by nonionic surfactant tyloxapol in rats. Toxicol Mech Methods 2020;30:73–80.
[20] Li Z, Huang J, Wang F, Li W, Wu X, Zhao C, et al. Dual targeting of bile acid receptor-1 (TGR5) and farnesoid X receptor (FXR) prevents estrogen-dependent bone loss in mice. J Bone Miner Res 2019;34:765–76.
[21] Chen K, Yan Z, Wang Y, Yang Y, Cai M, Huang C, et al. Shikonin mitigates ovariectomy-induced bone loss and RANKL-induced osteoclastogenesis via TRAF6-mediated signaling pathways. Biomed Pharmacother 2020;126:110067.
[22] Luo J, Yang Z, Ma Y, Yue Z, Lin H, Qu G, et al. LGR4 is a receptor for RANKL and negatively regulates osteoclast differentiation and bone resorption. Nat Med 2016;22:539–46.
[23] Luo J, Zhou W, Zhou X, Li D, Weng J, Yi Z, et al. Regulation of bone formation and remodeling by G-protein-coupled receptor 48. Development 2009;136:2747–56.
[24] Li C, Yang Z, Li Z, Ma Y, Zhang L, Zheng C, et al. Maslinic acid suppresses osteoclastogenesis and prevents ovariectomy-induced bone loss by regulating RANKL-mediated NF-κB and MAPK signaling pathways. J Bone Miner Res 2011;26:644–56.
[25] Sun L, Vukicevic S, Baliram R, Yang G, Sendak R, McPherson J, et al. Intermittent recombinant TSH injections prevent ovariectomy-induced bone loss. Proc Natl Acad Sci U S A 2008;105:4289–94.
[26] Asagiri M, Takayanagi H. The molecular understanding of osteoclast differentiation. Bone 2007;40:251–64.
[27] Zhu M, Liu H, Sun K, Liu J, Mou Y, Qi D, et al. Vinpocetine inhibits RANKL-induced osteoclastogenesis and attenuates ovariectomy-induced bone loss. Biomed Pharmacother 2020;123:109769.
[28] Han J, Gao W, Su D, Liu Y. Gypenoside inhibits RANKL-induced osteoclastogenesis by regulating NF-κB, AKT, and MAPK signaling pathways. J Cell Biochem 2018;119:7310–8.
[29] Krum SA, Brown M. Unraveling estrogen action in osteoporosis. Cell Cycle 2008;7:1348–52.
[30] Yoon KH, Cho DC, Yu SH, Kim KT, Jeon Y, Sung JK. The change of bone metabolism in ovariectomized rats : analyses of MicroCT scan and biochemical markers of bone turnover. J Korean Neurosurg Soc 2012;51:323–7.
[31] Thompson DD, Simmons HA, Pirie CM, Ke HZ. FDA Guidelines and animal models for osteoporosis. Bone 1995;17:125S–33S.
[32] Rissanen JP, Halleen JM. Models and screening assays for drug discovery in osteoporosis. Expet Opin Drug Discov 2010;5:1163–74.
[33] Iwaniec UT, Yuan D, Power RA, Wronski TJ. Strain-dependent variations in the response of cancellous bone to ovariectomy in mice. J Bone Miner Res 2006;21:1068–74.
[34] Klinck J, Boyd SK. The magnitude and rate of bone loss in ovariectomized mice differs among inbred strains as determined by longitudinal in vivo micro-computed tomography. Calcif Tissue Int 2008;83:70–9.